PHYSICAL REVIEW B **76**, 241404(R) (2007)

Order-disorder phase transition of the Cu(001) surface under equilibrium oxygen pressure

H. Iddir,[1] D. D. Fong,[1,*] P. Zapol,[1,2,†] P. H. Fuoss,[1] L. A. Curtiss,[1,2] G.-W. Zhou,[1,‡] and J. A. Eastman[1]
[1]*Materials Science Division, Argonne National Laboratory, Argonne, Illinois 60439, USA*
[2]*Chemical Sciences and Engineering Division, Argonne National Laboratory, Argonne, Illinois 60439, USA*
(Received 20 November 2007; published 27 December 2007)

In situ surface x-ray scattering is used to determine the stable oxygen-induced surface structure on Cu(001) at high temperatures and under equilibrium oxygen pressure. The structure is composed of a $c(2\times2)$-O adlayer atop a randomly 3/4-filled Cu layer for temperatures between 473 and 1000 K. Below 473 K, the vacancies in the topmost Cu layer order to form a $(2\sqrt{2}\times\sqrt{2})R45°$ missing row structure. This order-disorder transition is confirmed by first-principles calculations.

DOI: 10.1103/PhysRevB.76.241404 PACS number(s): 68.35.Fx, 68.47.De, 81.65.Mq, 82.65.+r

Equilibrium structures of metal surfaces in reactive environments determine their catalytic and other properties. Past studies of the relationships between the atomic structure of the catalyst and its catalytic activity and selectivity have been primarily carried out near room temperature and in ultrahigh vacuum, conditions far removed from the typical high-pressure flow environment of industrial catalysts. Recent work, however, has shown that the surface structure of operational catalysts can vary strongly with environment because of the pressure and temperature dependence of the surface free energy.[1–9] Indeed, there is growing evidence that some catalytic reactions previously ascribed to pure metal surfaces are actually effected by oxide surface phases.[1–3] To better understand catalytic reactions, it is imperative to both identify and characterize the atomic structure of all phases present on metal surfaces at elevated temperatures and pressures.

Copper catalysts are heavily used in methanol and formaldehyde synthesis, two reactions in which oxygen adsorption is an important intermediate step.[10–14] Previous low pressure investigations of Cu (001) surfaces found that as the oxygen coverage approaches one-half monolayer (θ=0.5 ML), the surface reconstructs to form a $(2\sqrt{2}\times\sqrt{2})R45°$ structure, where oxygen atoms adsorb to every other fourfold hollow site, and every fourth $\langle 100\rangle$ row of the uppermost Cu atoms is missing.[15,16] These structural changes can have profound implications on the catalytic turnover rate since surface reactivity is closely tied to surface morphology and induced strains.[17] A necessary step toward understanding the catalytic behavior of Cu is the characterization of surfaces under equilibrium controlled temperature and oxygen partial pressure conditions.

In this Rapid Communication, we present a structural investigation of Cu(001) surfaces at oxygen partial pressures P_{O_2} from 10^{-10} to 10^{-4} Torr and temperatures T from 300 to 1000 K, under flowing conditions. We use *in situ* synchrotron x-ray scattering to demonstrate that between 473 and 1000 K, the stable surface structure is comprised of a $c(2\times2)-$O adlayer atop a 3/4-filled Cu layer. Below 473 K, vacancies in the topmost Cu layer order to form the previously observed missing row $(2\sqrt{2}\times\sqrt{2})R45°$ structure. Density functional theory (DFT) calculations were performed to determine the relative stability of these structures.

The experiments were carried out at the Advanced Photon Source, Sector 12-ID-B, employing a specially designed reaction chamber mounted on an eight-circle (Psi-*c*) diffractometer. The chamber allows the study of samples from 300 to 1000 K in controlled P_{O_2}.[18] The samples are 200-nm-thick Cu (001) films grown on $SrTiO_3$(001) substrates by electron-beam evaporation.[18,19] After entering the reaction chamber, the samples are annealed at 973 K for 2 h in Ar-2% H_2 and then are cooled to the desired temperature for study. The films are fully strain relaxed, with a typical mosaic spread of 0.1° and a RMS roughness of 0.4 nm, as measured by *ex situ* atomic force microscopy. Scattering measurements were performed with 24 keV x rays, with incidence and exit angles set at the critical angle (0.14°) or at 0.5°. Reciprocal lattice units (rlu) are referenced to the primitive Cu surface unit cell throughout this Rapid Communication.

Examination of the in-plane scattering pattern at $L\approx0$ under different P_{O_2} and T allows determination of the surface phase diagram, as shown in Fig. 1(a). We find three distinct surface phases having 1×1, $c(2\times2)$, and $(2\sqrt{2}\times\sqrt{2})R45°$ symmetries. Above 473 K, increasing the P_{O_2} above $\sim10^{-8}$ Torr leads to a decrease in the intensity of the 100 and other integer-order positions along the crystal truncation rods (CTRs). This is expected for O adsorption onto the Cu fourfold hollow sites.[16] Shortly after adsorption, superstructure rods (SRs) appear at the $\frac{1}{2}$-order positions, as exemplified by the $\frac{1}{2}\frac{1}{2}0$ peak in Fig. 1(b). These SRs are consistent with the ordering of 0.5 ML of adsorbed O in a $c(2\times2)$ arrangement. The narrow width of the $\frac{1}{2}\frac{1}{2}0$ peak indicates that the $c(2\times2)-$O adlayer is well ordered, with a minimum domain size of $\sim$260 nm. After stabilization of the SR intensities, subsequent T and P_{O_2} changes within the $c(2\times2)$ phase field show little effect on peak intensities or shapes. The resulting surface structure in this pressure regime is therefore stable for $\theta\sim0.5$ ML. P_{O_2} larger than 10^{-4} Torr results in the nucleation and growth of Cu_2O (001) islands[18] and the gradual disappearance of the oxygen-adsorbed surface structure. Reduction of the P_{O_2} below the $c(2\times2)$ nucleating pressure also has little effect on peak intensities, indicating that the pressure boundary between the 1×1 and $c(2\times2)$ structures is hysteretic. At sufficiently high T and low P_{O_2}, oxygen desorbs from the surface.

To solve the $c(2\times2)$ surface structure, we measured the

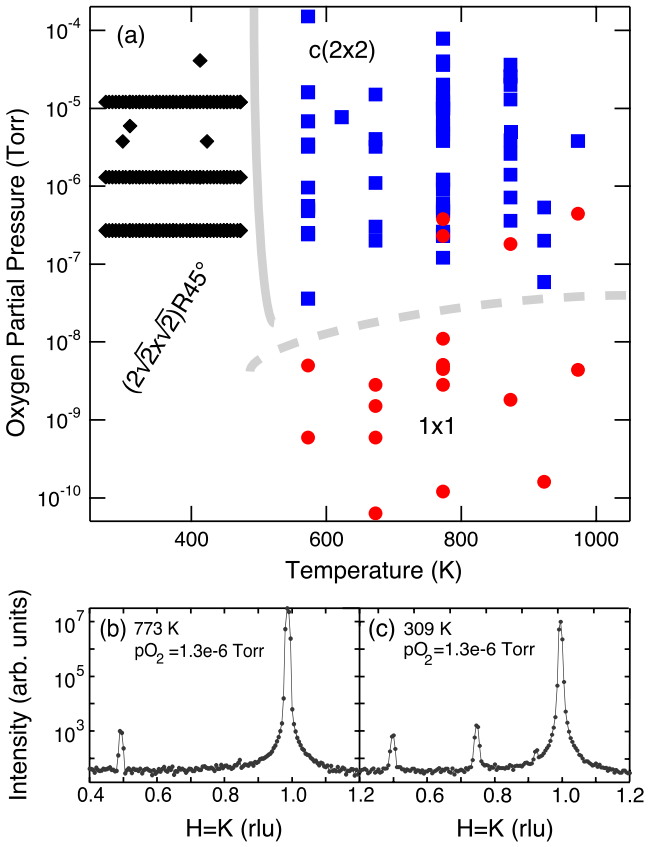

FIG. 1. (Color online) (a) Surface phase diagram for Cu(001)-O. The solid line is an equilibrium phase boundary between the $(2\sqrt{2}\times\sqrt{2})R45°$ and $c(2\times2)$ surface phases. The dashed line is the hysteretic boundary for oxygen adsorption and desorption. Data points are shown with symbols. (b), (c) Characteristic in-plane scans ($L\approx0$) along the $H=K$ direction of the $c(2\times2)$ and (22×2) $R45°$ reconstructions are shown in (b) and (c), respectively.

integrated intensities of seven SRs and four CTRs, for a sample at 3.8×10^{-6} Torr and 773 K. Standard geometrical, Lorentz, and polarization corrections were used,[20] and the structure was refined according to the usual procedures.[21] Four smaller data sets taken on other samples at similar T and P_{O_2} are in good agreement with the results reported here, differing primarily by the overall scale factor.

The absence of intensity at the $\frac{1}{4}$-order reflections rules out the $(2\sqrt{2}\times\sqrt{2})R45°$ missing row structure. A simple $c(2\times2)-O$ adlayer model provides reasonable agreement with the intensity of the SRs. However, the agreement was not satisfactory when CTR intensities were also included in the refinement. Assuming the oxygen atoms to be adsorbed as a $c(2\times2)-O$ adlayer in the fourfold hollow sites, we focused on possible structures for the underlying Cu layer. The large intensity reduction of the CTRs during adsorption suggests the loss of Cu atoms in the topmost layer. Allowance for this possibility produced the best-fit structure with a reduced $\chi^2=1.4$ for a top-layer occupancy of 3/4. Other fitting parameters included the Debye-Waller factors for oxygen and the topmost Cu atoms, the oxygen surface coverage, and a scale factor. The resulting structure is shown in Fig. 2(a), where 25% of the topmost Cu atoms are replaced with

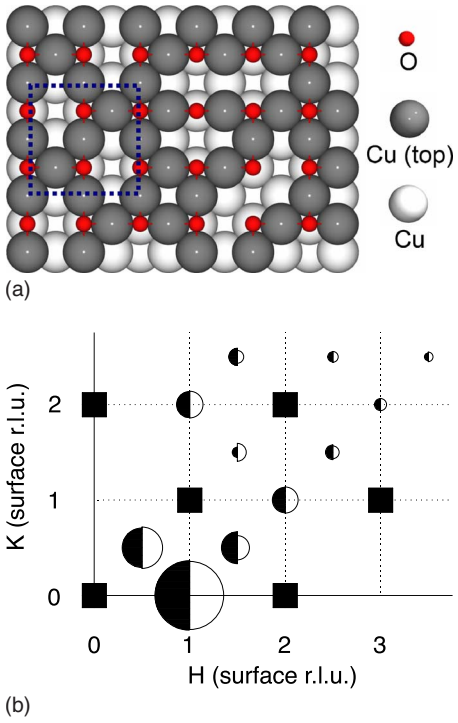

FIG. 2. (Color online) (a) Illustration of the $c(2\times2)$ structure with 1/4 ML disordered Cu vacancies. Dashed square shows $(2\sqrt{2}\times2\sqrt{2})$ surface cell chosen as a local representation of the structure for DFT calculations (spaced vacancy structure). (b) Structure factors for the $c(2\times2)$ reconstruction, plotted vs reciprocal space indices H and K. Areas of filled and open half circles are proportional to observed and calculated structure factors, respectively. Filled squares are bulk reflections.

randomly distributed vacancies. Comparison between the calculated structure factors from this model and the measured structure factors is shown in Fig. 2(b). When the $c(2\times2)$ surface is cooled below 473 K, $\frac{1}{4}$-order reflections, such as the $\frac{3}{4}\frac{3}{4}0$ in Fig. 1(c), appear. Figure 3 shows the T dependence of this peak under different P_{O_2}. In the vicinity of the transition, the intensity of the $\frac{3}{4}\frac{3}{4}0$ is fully reversible

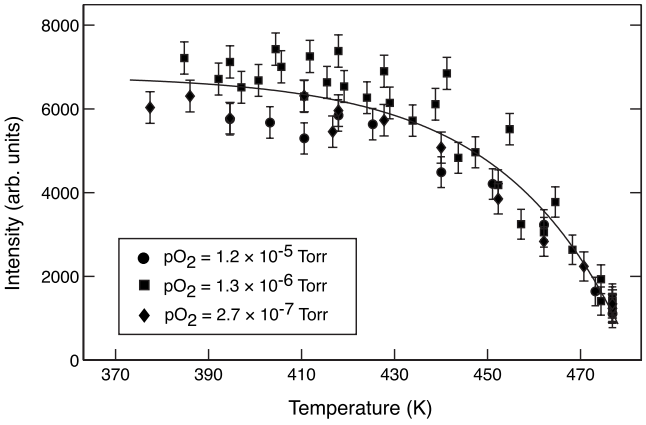

FIG. 3. Temperature dependence of the $\frac{3}{4}\frac{3}{4}0$ peak intensity under different oxygen partial pressures. Solid line is the best fit to a 2D Ising model (Ref. 22).

with temperature and shows little hysteresis. The $\frac{1}{4}$-order reflections are consistent with those of the previously determined $(2\sqrt{2}\times\sqrt{2})R45°$ missing row structure,[15] demonstrating that this is an order-disorder transition, with a random distribution of 1/4 ML Cu vacancies in the topmost atomic plane ordering themselves along every fourth ⟨100⟩ row below 473 K.

To investigate the relative stability of the surface phases, calculations were performed using DFT as implemented in VASP[23] with Perdew-Wang exchange-correlation functionals[24] and projected augmented wave potentials.[25] Cu (001) surfaces were modeled using periodic five-layer slabs with the two bottom layers fixed at the theoretical bulk value (3.636 Å) and a vacuum region of 12.36 Å. To compare the stability of the $c(2\times2)-O$ adlayer with different Cu vacancy concentrations in the topmost layer, we have optimized these structures for 0, 12.5, 25, and 37.5 % concentrations using $(2\sqrt{2}\times2\sqrt{2})$ supercells and several initial structures for each concentration. The calculated lowest formation energies per surface vacancy are −0.06, −0.21, and −0.03 eV (using the chemical potential of bulk Cu) for the 12.5, 25, and 37.5 % concentrations, respectively. This results in surface energy differences of −0.02, −0.13, and −0.03 J/m^2 as compared to a surface with no vacancies, indicating that the stable structure has 25% Cu vacancy concentration. For this concentration, the calculated total energy differences among several possible vacancy configurations [and with the same $c(2\times2)-O$ adlayer] demonstrate the missing row structure as the stable phase at low temperatures. Many previous experimental observations and theoretical calculations[26–30] have considered the transition from the $c(2\times2)$ structure with no Cu vacancies to the missing row structure with an increase in oxygen concentration. Our results are in agreement with these studies in that the $(2\sqrt{2}\times\sqrt{2})R45°$ missing row structure is stable for an oxygen coverage of $\theta=0.5$ ML. Our study is aimed at the elucidation of temperature-dependent surface phase transitions at fixed oxygen coverage. The missing row configuration (Fig. 4) is lower in total energy than the spaced-vacancy structure [Fig. 2(a) box], by 0.13 eV and than the clustered-vacancy configuration (Fig. 4) by 0.16 eV. The small difference between these two values shows that repulsive interactions of neighboring vacancies are weak, validating the assumption that the calculated vacancy formation energy in the spaced-vacancy configuration is the same as that in the random vacancy configuration.

To compare the stability of the random vacancy phase to that of the missing row structure with the same vacancy concentration of 25%, we have calculated the free energy differences as the total energy differences given above and T-dependent configurational entropy term calculated as $S=-k\left[\frac{1-\Theta}{\Theta}\ln(1-\Theta)+\ln(\Theta)\right]$, where Θ is the vacancy concentration. Comparison of the free energies shows that the missing row configuration is stable up to 650 K, above which temperature the random phase structure is more stable. Calculated surface free energies for other copper vacancy concentrations are higher than either of the 25% vacancy structures in the whole temperature range from 0 to 1200 K. These results are in qualitative agreement with our observed

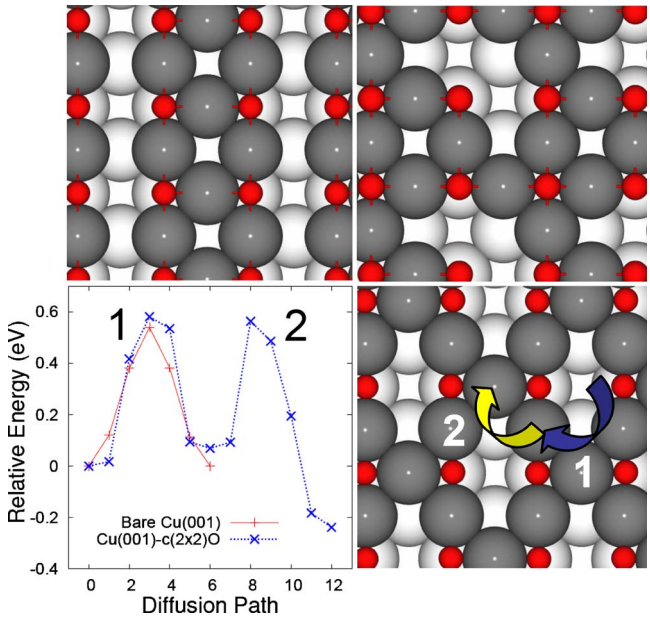

FIG. 4. (Color online) Top: Missing row (left) and clustered (right) Cu vacancy configurations. Bottom left: Cu vacancy diffusion energy barriers on bare and 50% O-covered Cu(001) surfaces. The minimum between the barriers (NEB image 6) corresponds to clustered vacancies. Bottom right: Diffusion paths 1 and 2 of the Cu vacancy.

phase transition temperature of 473 K, and show that the order-disorder transition is indeed entropy driven.

The transition from a high-temperature random vacancy phase to the $(2\sqrt{2}\times\sqrt{2})R45°$ ordered phase and vice versa occurs through Cu vacancy diffusion. To show that such a transition is not only thermodynamically favorable, but also feasible from the kinetic point of view, the energy barrier for vacancy diffusion was determined and compared to the barrier for the bare surface. It was previously shown that surface vacancy diffusion on Cu(001) is very fast[31] implying a low activation energy for vacancy diffusion on the bare surface. Using the nudged elastic band method,[32] we calculated the energy barrier for the diffusion of a surface Cu vacancy on the bare Cu (001) surface to be 0.54 eV, as compared to 0.42 eV in previous work.[33] To model the order-disorder transition, we calculated the energy barriers for vacancy diffusion along paths that correspond to the transition from a spaced-vacancy phase (taken as a local representation of the random phase, Fig. 2) to the $(2\sqrt{2}\times\sqrt{2})R45°$ phase. In the presence of the oxygen adlayer, the energy barrier remained almost the same, 0.56 and 0.53 eV for the diffusion along path 1 and path 2, respectively (Fig. 4). This result is counterintuitive since one expects that the oxygen adlayer will increase the coordination of the topmost Cu atoms and thus will stabilize the Cu structure, resulting in higher energy barriers. The similarity of energy barriers of the surface with oxygen adlayer to those on the bare surface suggests that the diffusion of surface vacancies is barely affected by the presence of oxygen. Oxygen also retains its $c(2\times2)$ superstructure during Cu vacancy diffusion. Hence there is no kinetic

hindrance to the order-disorder transition that we have observed.

In summary, we find a temperature-driven order-disorder transition in the 1/4 ML Cu vacancy structure on a 0.5 ML oxygen covered (001) surface. Both *in situ* surface x-ray scattering and DFT calculations indicate vacancy disordering from the missing row structure at elevated temperatures. This phase transition is likely to have profound implications on catalytic processes involving oxidative reactions such as the partial oxidation of methane or methanol as well as the development of subsurface oxygen for bulk oxide formation. Such phase transitions are likely to occur in other systems with strong adsorbate interactions and partially filled top metal layers.

This work was supported by DOE BES under Contract No. DE-AC02-06CH11357.

*fong@anl.gov

†zapol@anl.gov

‡Present address: Department of Mechanical Engineering, Binghamton University, State University of New York, Binghamton, NY 13902.

[1] H. Over, Y. D. Kim, A. P. Seitsonen, S. Wendt, E. Lundgren, M. Schmid, P. Varga, A. Morgante, and G. Ertl, Science **287**, 1474 (2000).

[2] B. L. M. Hendriksen and J. W. M. Frenken, Phys. Rev. Lett. **89**, 046101 (2002).

[3] M. D. Ackermann *et al.*, Phys. Rev. Lett. **95**, 255505 (2005).

[4] H. Over and A. P. Seitsonen, Science **297**, 2003 (2002).

[5] E. Lundgren, J. Gustafson, A. Mikkelsen, J. N. Andersen, A. Stierle, H. Dosch, M. Todorova, J. Rogal, K. Reuter, and M. Scheffler, Phys. Rev. Lett. **92**, 046101 (2004).

[6] B. L. M. Hendriksen, S. C. Bobaru, and J. W. M. Frenken, Top. Catal. **36**, 43 (2005).

[7] A. Stierle, N. Kasper, H. Dosch, E. Lundgren, J. Gustafson, A. Mikkelsen, and J. N. Andersen, J. Chem. Phys. **122**, 044706 (2005).

[8] K. Reuter, in *Nanocatalysis*, edited by U. Heiz and U. Landman (Springer, Berlin, 2007).

[9] E. Lundgren, A. Mikkelsen, J. N. Andersen, G. Kresse, M. Schmid, and P. Varga, J. Phys.: Condens. Matter **18**, R481 (2006).

[10] M. Bowker, Top. Catal. **3**, 461 (1996).

[11] T. Schedel-Niedrig, M. Hävecker, A. Knop-Gericke, and R. Schlögl, Phys. Chem. Chem. Phys. **2**, 3473 (2000).

[12] J. R. B. Gomes and J. A. N. F. Gomes, Surf. Sci. **471**, 59 (2001).

[13] H. Bluhm, M. Hävecker, A. Knop-Gericke, E. Kleimenov, R. Schlögl, D. Teschner, V. I. Bukhtiyarov, D. F. Ogletree, and M. Salmeron, J. Phys. Chem. B **108**, 14340 (2004).

[14] S. Sakong and A. Gross, J. Catal. **231**, 420 (2005).

[15] I. K. Robinson, E. Vlieg, and S. Ferrer, Phys. Rev. B **42**, 6954 (1990).

[16] M. Kittel *et al.*, Surf. Sci. **470**, 311 (2001).

[17] M. Mavrikakis, B. Hammer, and J. K. Nørskov, Phys. Rev. Lett. **81**, 2819 (1998).

[18] J. A. Eastman, P. H. Fuoss, L. E. Rehn, P. M. Baldo, G.-W. Zhou, D. D. Fong, and L. J. Thompson, Appl. Phys. Lett. **87**, 051914 (2005).

[19] A. J. Francis, Y. Cao, and P. A. Salvador, Thin Solid Films **496**, 317 (2006).

[20] E. Vlieg, J. Appl. Crystallogr. **30**, 532 (1997).

[21] *International Tables for X-ray Crystallography*, edited by J. S. Kaspar and K. Lonsdale (Kynoch, Birmingham, 1972), Vol. II.

[22] The temperature dependence of the order-disorder transition shown in Fig. 3 is consistent with Onsager's critical exponent of 1/8 for a 2D Ising universality class. This result agrees with our theoretical finding of weak vacancy-vacancy interaction, since considerable second neighbor interactions change the critical exponent (Ref. 34).

[23] G. Kresse and J. Furthmuller, Phys. Rev. B **54**, 11169 (1996).

[24] J. P. Perdew and Y. Wang, Phys. Rev. B **45**, 13244 (1992).

[25] P. E. Blöchl, Phys. Rev. B **50**, 17953 (1994).

[26] K. W. Jacobsen and J. K. Nørskov, Phys. Rev. Lett. **65**, 1788 (1990).

[27] E. A. Colbourn and J. E. Inglesfield, Phys. Rev. Lett. **66**, 2006 (1991).

[28] S. Stolbov and T. S. Rahman, Phys. Rev. Lett. **89**, 116101 (2002).

[29] I. Merrick, J. E. Inglesfield, and H. Ishida, Surf. Sci. **551**, 158 (2004).

[30] M. J. Harrison, D. P. Woodruff, J. Robinson, D. Sander, W. Pan, and J. Kirschner, Phys. Rev. B **74**, 165402 (2006).

[31] R. van Gastel, E. Somfai, S. B. van Albada, W. van Saarloos, and J. W. M. Frenken, Phys. Rev. Lett. **86**, 1562 (2001).

[32] G. Mills, H. Jonsson, and G. K. Schenter, Surf. Sci. **324**, 305 (1995).

[33] G. Boisvert and L. J. Lewis, Phys. Rev. B **56**, 7643 (1997).

[34] K. Binder and D. P. Landau, Phys. Rev. B **21**, 1941 (1980).